XVII IMEKO World Congress
Metrology in the 3rd Millennium
June 22- 27, 2003, Dubrovnik, Croatia

THE INFLUENCE OF SURFACE INCLINATION ON THE CALIBRATION OF SURFACE TEMPERATURE SENSORS

Emese András

National Office of Measures (OMH), Budapest, Hungary

Abstract - The OMH has developed a reference surface temperature apparatus for the calibration of contact surface temperature sensors under a variety of conditions. This article describes the dependence of temperature error on the inclination of a heated surface and studies the sources of these deviations for various surface temperatures and sensor types. The effect of surface inclination has not been investigated before but has been found significant, particularly because of its industrial relevance.

Keywords: temperature surface heat-transmission

1. INTRODUCTION

Our laboratory was among the first ones having developed a reference surface temperature apparatus using electrical heating. Its temperature range is presently the largest in the world: from ambient temperature to 600 °C. The reference walls are exchangeable: they can be metals or insulating materials embracing a large range of thermal conductivity values.

The principle of surface sensor calibration is to compare the standard surface temperature with that determined by a surface sensor directly applied to one of the reference surfaces. The calibration procedure used involves the determination of the surface temperature by extrapolation before applying the sensor [1].

There are various sources of errors and uncertainties associated with the calibration of surface sensors.

Bilateral comparisons carried out in this field between PTB and OMH and between BNM-LNE and OMH showed a good general consistency of the results and have met industrial need in reducing uncertainty [1].

At moment OMH is co-ordinating the Euromet Project 635, which is a comparison of the reference surface temperature apparatus at eleven NMIs by comparison of transfer surface temperature standards. The technical co-operation activities consists of the exchange of experience and comparison concerning the development of the basic apparatus, requirements and procedures for traceability, influence of the thermophysical properties of surfaces, etc.

In case of temperature measurements made on the surfaces of solid bodies, the heat flux depends, on the one hand, on the temperature difference between the solid body and the ambient, on the other hand, on the heat transmission coefficient (which expresses the effect of conduction, convection and radiation).

In order to determine the temperature of a given surface with higher precision, the value indicated by a surface temperature sensor must be corrected. This correction depends mainly of three factors:

- *Properties of the heated wall:* the geometrical and thermophysical characteristics of the material, the temperature of the wall, the quality of the surface (roughness, oxidation);
- *Influence of the surface sensor:* type, geometrical and thermophysical characteristics of the sensor [2];
- *Heat transfer effects:* he quality of the heat transfer at the interfaces surface-sensor and ambient-thermometer influences the difference between the temperature of the surface of the heated solid body and that of the contact surface of the sensor.

This correction is the subject of this paper.

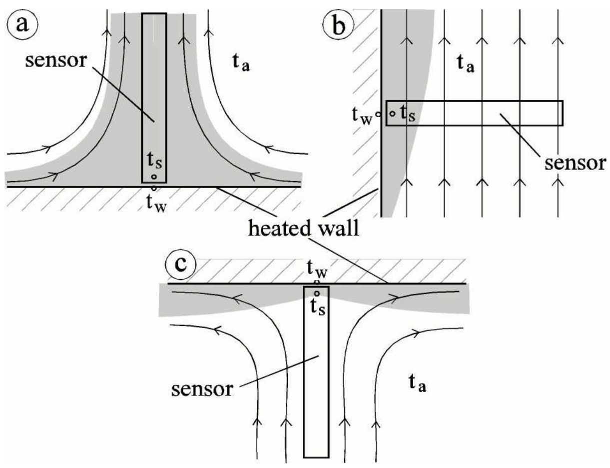

Fig. 1. Extreme positions of the surface

The main portion of the resistance to heat transfer is usually concentrated in a thin layer immediately adjacent to the wall surface (thermal boundary layer).
Heat transfer is essentially an interplay of heat conduction from the solid surface and energy transport by the moving fluid within this layer. Hence, the heat transfer depends essentially on the thickness and the characteristics of this boundary-layer (Fig. 1.).

The greyed elements in Fig. 1 represent the thermal boundary-layer, whose temperature is much higher than the ambient temperature. It can be seen that the structure of the boundary-layer depends strongly on the surface inclination and this is the motivation for this paper.
In case of calibration for a horizontal surface (α=0°) (Figure 1a) a free flow is formed along the sensor and the temperature in the boundary-layer is higher than the ambient temperature (ta). In case of calibration for a vertical surface (α=90°) (Figure 1b), vertical free flow is formed around the sensor. The temperature changes little except in the vicinity of the surface, in the boundary-layer. A portion of the sensor is located in this warm boundary-layer. In case of calibration for a horizontal surface (α=180°) (Figure 1c) a free flow is formed along the sensor and its temperature is the same as the ambient temperature.

This paper tries to present and interpret measurement results, provide a physical explanation and quantify the above-mentioned effects.

2. CALIBRATION METHOD FOR DIFFERENT SURFACE INCLINATIONS

The reference surface temperature apparatus used for these calibrations is presented in Fig. 2.

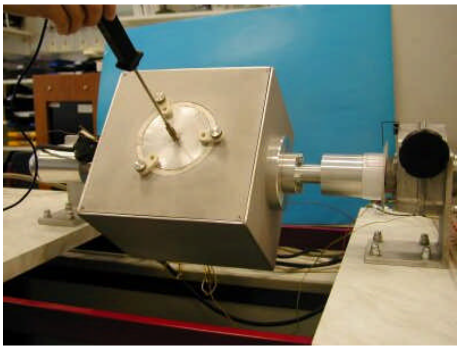

Fig. 2. Reference surface temperature apparatus at OMH

These surface temperature measurements were effectuated in the temperature range between 100°C and 400°C, using a Testo temperature indicator Type 945 with three different sensors (Fig 3):

Fig. 3. Different surface sensors

- sensor s1, type Testo 0602.0392, with sprung cross thermocouple strip
- sensor s2, type Omega 88010K, with sprung thermocouple strip
- sensor s3, type Testo 0602.0692, with a small, non-sprung measuring head

The ambient temperature was 23 °C. The flat heated wall was made of aluminium with a thermal conductivity coefficient λ=230W/m·K. The heated plane wall had a diameter of 100 mm and a thickness of 20 mm.

The calibration procedure starts with the determination of the surface temperature by extrapolation before applying the sensor [1]. The surface sensor is applied manually on the aluminium plate.

3. MEASUREMENT RESULTS

Surface temperatures were measured with three types of surface sensors, for three different temperatures between 100°C and 400°C and for seven different angles of the heated reference wall between 0° and 180°.

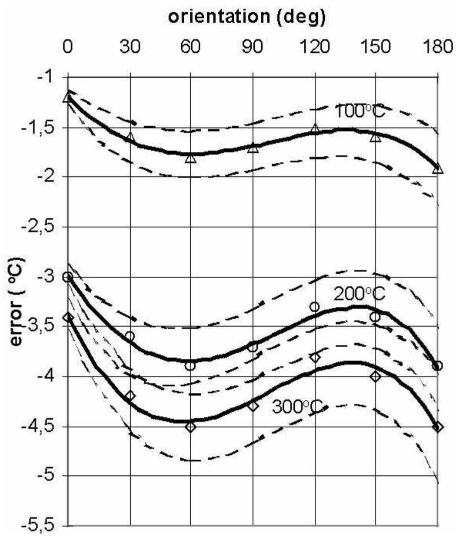

Fig. 4. Calibration curve of sensor s1

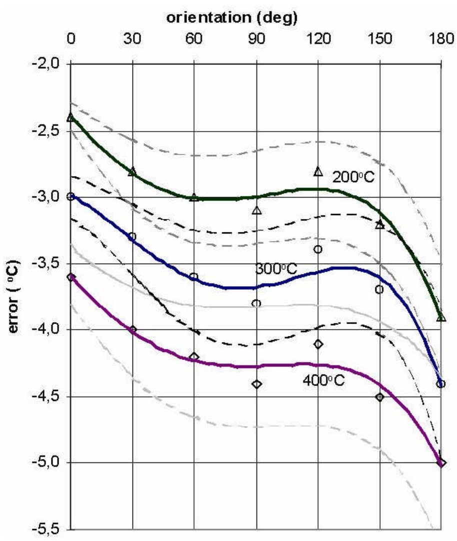

Fig. 5. Calibration curve of sensor s2

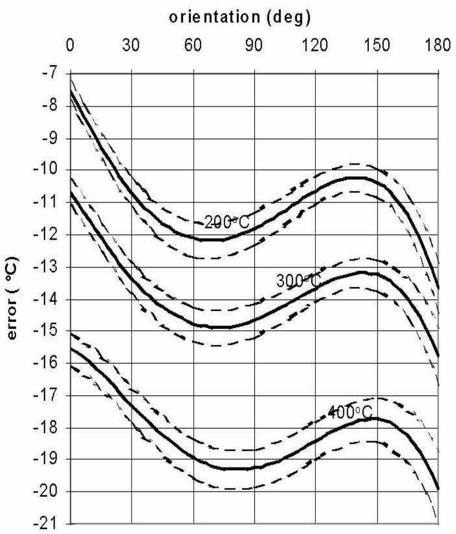

Fig. 6. Calibration curve of sensor s3

The achieved results show a significant difference of the measurement error due to the variation of the reference surface inclination (Fig. 4, 5, 6.).

The points presented in each diagram are mean values of twenty measurements, for a given temperature and angle. The continuous curves are trend-lines of forth-degree functions. Interrupted lines embed each of the uncertainty-band.

Can be seen that each curve has the same character, independently of the surface temperature and of the sensor-construction.

4. ANALYSIS OF THE MEASUREMENT RESULTS

4.1. Theoretical model of the surface sensor

The surface sensor is considered as a heated hollow bar with finite length, having constant temperature t_w at one end and which heat is flowing to an infinite field with constant temperature t_a. This heat transfer is effectuated by conduction, convection and radiation.

Considering the surface sensor as a hollow bar with diameter d_s, thickness s of its wall, length h_s, can be determined the following expressions: the area $A_s = p \cdot d_s \cdot s$ of heat-conduction and the perimeter $K_s = p \cdot d_s$. Introducing the relation:

$$a = \sqrt{\frac{a_s \cdot K_s}{l_s \cdot A_s}} \qquad (1)$$

, where a_s is the heat transmission coefficient from bar to ambient and l_s is the coefficient of thermal conductivity of the bar. The outlet heat flow by convection from the bar can be calculated with the aid of the following formulas [3], [4]:

$$Q_k = l_s \cdot A_s \cdot a \frac{e^{a \cdot h_s} - e^{-a \cdot h_s}}{e^{a \cdot h_s} + e^{-a \cdot h_s}} (t_w - t_a) \qquad (2)$$

a_s is obtained from the Nusselt number:

$$Nu = \frac{a_s \cdot X}{l_a} \qquad (3)$$

, where X is a typical geometrical dimension and l_a is the thermal conductivity coefficient of the fluid. Moreover, the Nusselt number can be written [5]:

$$Nu = c \cdot (Gr \cdot Pr)^n \cdot K \qquad (4)$$

, where c, n and K are factors depending on the geometry of the surface and its inclination relative to the gravitational field, Gr is the Grashof number and Pr is the Prandtl number. Taking into consideration the relations (3) and (4), the heat transmission coefficient can be calculated with the following equation:

$$a_s = \frac{l_a}{X} \cdot c \cdot (Gr \cdot Pr)^n \cdot K \qquad (5)$$

Practically, the factors *c*, *n*, *K* and *X* are given in [3] in two extreme situations. In case of a vertical bar $X = h_s$, $c = 0{,}686$, $n = 0{,}25$ and $K = \left(\frac{Pr}{1 + 1{,}05 \cdot Pr}\right)^{0{,}25}$. For a horizontal bar $X = d_s$, $c = 0{,}47$, $n = 0{,}25$ and $K = 1$.

The outlet heat flow from the bar by radiation can be expressed [3], [4]:

$$Q_R = s \cdot A \cdot A_R \cdot e_R \cdot (T_{ms}^4 - T_a^4) \qquad (6)$$

, where s is the Boltzmann constant, A_R is the area of the radiating surface, e_R is the emissivity coefficient, T_{ms} is the mean absolute temperature of the surface and T_a is the absolute temperature of the ambient.

The total outlet heat flow is:

$$Q_t = Q_k + Q_R \qquad (7)$$

The calculations carried out for the sensor s1, using the following parameters:
$d_s = 4mm$, $s = 0{,}5mm$, $h_s = 150mm$, $l_s = 30\,W/m \cdot K$ and $e_R = 0{,}25$ and $t_a = 23^\circ C$.

The calculation results are presented in Table I., where the index *v* is used for the vertically positioned sensor and index *h* for the horizontal one.

TABLE I.

t [°C]	Q_{kv} [W]	Q_{kh} [W]	Q_R [W]	Q_{tv} [W]	Q_{th} [W]
100	0,306	0,448	0,130	0,436	0,579
200	0,758	1,110	0,379	1,137	1,489
300	1,231	1,802	0,746	1,977	2,548
400	1,714	2,510	1,265	2,980	3,775

4.2. Comparison of the theoretical and the measured deviations

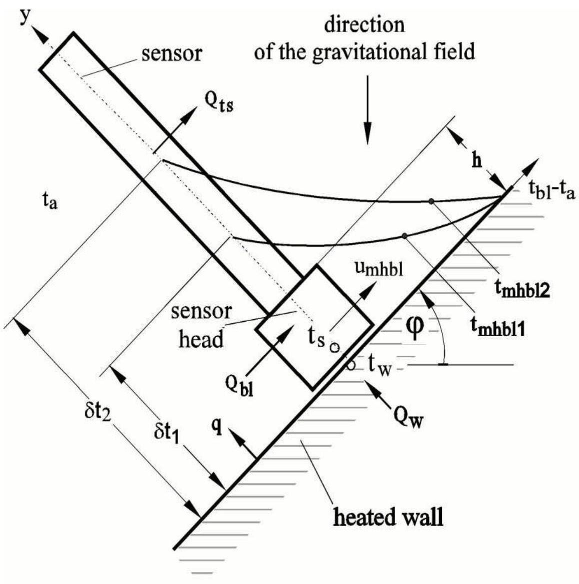

Fig. 7. Model of surface measurement

The measurement error is related to the temperature of the heated wall t_w and to the inclination angle j (Fig. 7.) and defined as:

$$dt_m = t_s - t_w \tag{8}$$

, where t_s is the temperature indicated by the thermometer. The measured temperature errors dt_m as a function of the angle j and for a given t_w is shown in Fig. 8.

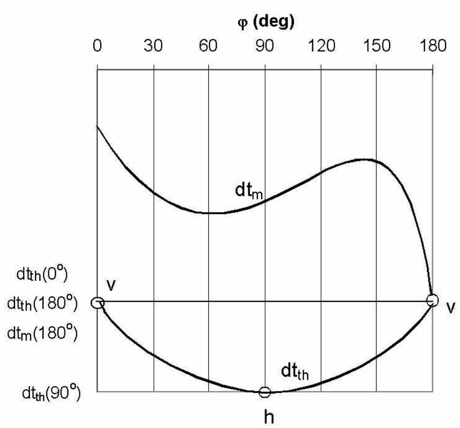

Fig. 8. Measured and theoretical temperature-errors as a function of the inclination angle

The flow developing near the heated wall deforms the temperature field of the ambient. In case of the extreme positions of the surface, this thermal boundary-layer can be seen in Fig. 1. It can be observed that the boundary-layer near the sensor-head is the most thin for $j = 180^\circ$, so in this point the theoretical curve can be connected to the curve of the measurement errors with good approximation:

$$dt_{\mathrm{th}}(180^\circ) = dt_m(180^\circ) \tag{9}$$

In the vertical position (v) of the sensor, the heat flow Q_{tv} can be written:

$$Q_{tv} = f_s \cdot dt_{\mathrm{th}}(180^\circ) \tag{10}$$

The factor f_s can be determined:

$$f_s = \frac{Q_{tv}}{dt_m(180^\circ)} \tag{11}$$

Moreover, the theoretical error can be written using the total heat flow Q_{th} related to t_w (Fig. 8.):

$$dt_{\mathrm{th}}(90^\circ) = \frac{Q_{\mathrm{th}}}{f_s} \tag{12}$$

This is a symmetrical curve with respect to the vertical $j = 90^\circ$ ($dt_{\mathrm{th}}(0^\circ) = dt_{\mathrm{th}}(180^\circ)$).

Mathematical formulae can be found in the specialised literature only for extreme angles. Considering the following equation:

$$dt_{\mathrm{th}} = a \cdot j^2 + b \cdot j + c \tag{13}$$

and knowing the pairs of values $\lfloor j = 0^\circ, dt_{\mathrm{th}}(0^\circ) \rfloor$, $\lfloor j = 90^\circ, dt_{\mathrm{th}}(90^\circ) \rfloor$ and $\lfloor j = 180^\circ, dt_{\mathrm{th}}(180^\circ) \rfloor$, the coefficients *a*, *b* and *c* can be calculated. The deviation ddt_{th} between the theoretical and the measured temperature error is:

$$ddt_{\mathrm{th}} = dt_m - dt_{\mathrm{th}} \tag{14}$$

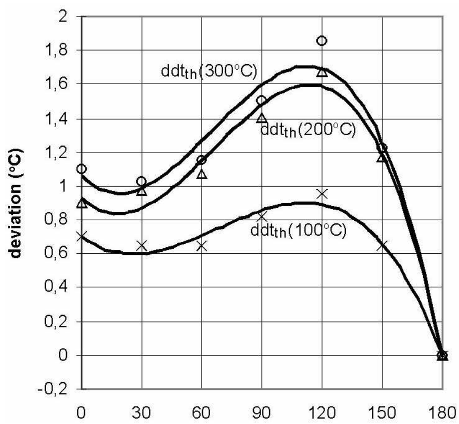

Fig. 9. Deviation of the theoretical temperature error from the measured one

Here the concrete calculations of dt_{th} and ddt_{th} for sensor *s*1 is presented, using (13) and (14) which can be seen in Fig.9. Considering the following equation:

$$ddt_{\mathrm{th}} = (180^\circ - j) \cdot (a_k + b_k \cdot j + c_k \cdot j^2) \tag{15}$$

, coefficients a_k, b_k and c_k can be calculated.

4.3. Physical interpretation of the difference between the theoretical and the measured deviations

The sensor-head of length *h* and for certain angle intervals also a part of the sensor-bar are situated in the thermal boundary-layer development along the heated wall (Fig. 7.). The temperature distribution in a thermal boundary-layer development along a flat plate can be written as [6]:

$$t_{bl} - t_a = (t_w - t_a)\cdot\left(1 - \frac{y}{\delta}\right)^2 \qquad (16)$$

, where δ is the thickness of the boundary-layer.

The heat-flow field and thermal boundary-layer developments, surrounding the heated wall and the sensor, are sketched for various angle intervals in Fig. 10 and Fig. 11.

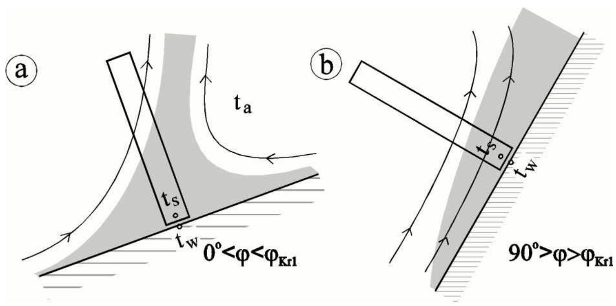

Fig. 10. Flow field and thermal boundary-layer in case of $\varphi \in [0^\circ,\ 90^\circ]$

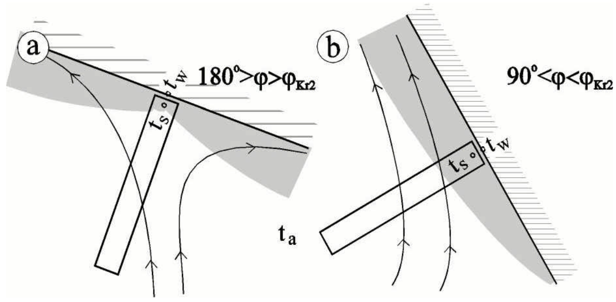

Fig. 11. Flow field and thermal boundary-layer in case of $\varphi \in [90^\circ,\ 180^\circ]$

Equation (16) is valid only in the $\varphi \in [\varphi_{kr1}, \varphi_{kr2}]$ interval.

In case of the sensor, the outlet heat flows should be equal with inlet heat flow. In particular, the heat flow through heated wall / sensor-head interface can be expressed:

$$Q_w = f \cdot dt_m \qquad (17)$$

, where $dt_m = t_s - t_w$ is the measurement error and f is the inverse value of the thermal resistance.

Due to the fact, that the sensor-head gets heat addition not only from the contact surface, but also from the thermal boundary-layer, the following relation is valid:

$$Q_{ts} = Q_w + Q_{bl} \qquad (18)$$

, where Q_{ts} is the outlet heat flow from the sensor-bar, Q_w and Q_{bl} are inlet heat flows from the contacted surface and from the boundary-layer respectively. Taking into consideration that

$$Q_{ts} = f \cdot dt_{\text{th}} \qquad (19)$$

and based on (17) and (18), it can be seen that the difference between theoretical and measured errors can be attributed to the boundary-layer:

$$\frac{Q_{bl}}{f} = dt_{\text{th}} - dt_m = -ddt_{\text{th}} \qquad (20)$$

Based on the analysis of the heat flow Q_{bl} as a function of the angle, the qualitative behaviour of ddt_{th} can be determined. The convective heat-flux Q_{wk} from the heated wall obeys [1] [2]:

$$Q_{wk}(\varphi = 0^\circ) \rangle\ Q_{wk}(\varphi = 90^\circ) \rangle\ Q_{wk}(\varphi = 180^\circ) \qquad (21)$$

Hence, the heat flow Q_{wk} can be expressed by a monotonically decreasing function (Fig. 12.)

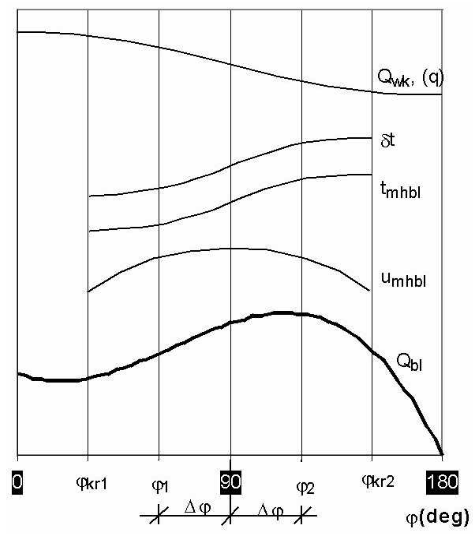

Fig. 12. Qualitative analysis of the heat transfer from the boundary layer to the sensor

As a consequence of the temperature distribution of the boundary-layer, the specific rate of heat flow q is inversely proportional with the thickness δ of the boundary-layer, therefore δ can be expressed with the aid of a monotonically increasing function in the interval $\varphi \in [\varphi_{kr1},\ \varphi_{kr2}]$. For symmetrical φ values with respect to 90° ($\varphi_1 = 90^\circ - \Delta\varphi$, $\varphi_2 = 90^\circ + \Delta\varphi$), is follows that $\delta_1 \langle\ \delta_2$. Fig. 7 shows that for the mean temperatures relative to the layer of thickness *h*, the following inequality is valid:

$$t_{mhbl2} \rangle\ t_{mhbl1} \qquad (22)$$

We have indicated t_{mhbl} a monotonically increasing function of φ (Fig. 12.).

The mean flow velocity u_{mhbl} relative to the layer of thickness *h* is the highest for $\varphi = 90^\circ$ (Fig. 12.).

The heat flow from the boundary-layer to the sensor-head is proportional with the velocity u_{mhbl} and with the temperature t_{mhbl} :

$$Q_{bl} \sim u_{mhbl} \cdot h \cdot t_{mhbl} \qquad (23)$$

It has been thus demonstrated that Q_{bl} is not symmetrical with respect to $j = 90^\circ$, explains the asymmetry of the ddt_{th}.

In particular the variation of Q_{bl} in the angle interval $j \in [0,\ j_{kr1}]$ can also be explained with the aid of Fig. 10. In case of $j = 0^\circ$, the whole sensor is immersed in the thermal boundary-layer (Fig. 1.). Increasing the angle j, a larger and larger part of the sensor-bar emerges from the boundary-layer. For this reason Q_{bl} is a monotonically increasing function of the angle interval. The variation of Q_{bl} in the interval $j \in [j_{kr2},\ 180^\circ]$ can be interpreted using Fig. 11. In the case of $j = 180^\circ$ (Fig. 3.), the cold air blows away the boundary-layer from the sensor-head, therefore $Q_{bl}(j = 180^\circ) \cong 0$. Thus, as seen in Fig. 11 that q_{bl} is a monotonically decreasing function of φ in this angle interval. In Fig. 12 we have obtained a $Q_{bl}(j)$ function similar to the $ddt_{\mathrm{th}}(j)$ function in Fig. 8.

5. CONCLUSIONS

Surface sensor measurements, compounded by considerable errors, which were not quantified, can nowadays be corrected by values determined during calibration.

One of these significant errors is estimated in this work. The measurement results prove unambiguously the influence of surface inclination on the measurement error.

In this first step of the investigations, a theoretical analysis has been carried out to estimate the temperature-error related to surface inclination.

These investigations led to a better approach of surface temperature measurements using contact sensors and improvements in the calibration methods and procedures.

REFERENCES

[1] R. Morice, E. András, E. Devin, T. Kovács, "Contribution for the calibration and the use of surface temperature sensors", Tempmeko Proceedings, vol. 2, pp.1111-1116, 2001.

[2] F. Bernhard, S. Augustin, H. Mammen, K.D. Sommer, E. Tegeler, M. Wagner, U. Demisch, "Calibration of contacting sensors for temperature measurements on surfaces", Tempmeko Proceedings, vol. 1, pp. 257-262, 1999.

[3] M.A. Mihejev, "Bases of practical calculations concerning the heat-transfer", "A hõátadás gyakorlati számításának alapjai" Tankönyvkiadó, Budapest, 1990.

[4] T. Környey, "Transmission of heat", "Hõátvitel", Mûegyetemi kiadó, Budapest, 1999.

[5] H. Y. Wong, "Heat transfer for engineers", Longman Group Limited, London, 1983.

[6] E. R. G. Eckert, R. M. Drake Jr., "Heat and Mass Transfer", Mc Graw - Hill Book Company, Inc., New York, Toronto, London, 1959.

AUTHOR: Emese András, Thermometry Division, National Office of Measures, 1124 Budapest, Hungary, phone: 36 1 4585963, fax: 36 1 4585927, E-mail: e.andras@omh.hu